Published in final edited form as:
Pain. 2009 November ; 146(1-2): 130–140. doi:10.1016/j.pain.2009.07.011.

Role of SIP30 in the development and maintenance of peripheral nerve injury-induced neuropathic pain

Yu-Qiu Zhang[1,2,*,¶], **Ning Guo**[1,5,*], **Guangdun Peng**[3,*], **Mei Han**[2], **Jeremy Raincrow**[5], **Chi-hua Chiu**[5], **Lique M. Coolen**[1], **Robert J. Wenthold**[4], **Zhi-Qi Zhao**[2,¶], **Naihe Jing**[3,¶], and **Lei Yu**[1,5,¶]

[1] Department of Cell Biology, Neurobiology and Anatomy, University of Cincinnati College of Medicine, Cincinnati, Ohio, USA

[2] Institute of Neurobiology, Institutes of Brain Science and State Key Laboratory of Medical Neurobiology, Fudan University, Shanghai, China

[3] Laboratory of Molecular Cell Biology and Key Laboratory of Stem Cell Biology, Institute of Biochemistry and Cell Biology, Shanghai Institutes for Biological Sciences, Chinese Academy of Sciences, Shanghai, China

[4] Laboratory of Neurochemistry, NIDCD, National Institutes of Health, Bethesda, Maryland, USA

[5] Department of Genetics and Center of Alcohol Studies, Rutgers University, Piscataway, New Jersey, USA

Abstract

Using the chronic constriction injury (CCI) model of neuropathic pain, we profiled gene expression in the rat spinal cord, and identified SIP30 as a gene whose expression was elevated after CCI. SIP30 was previously shown to interact with SNAP25, but whose function was otherwise unknown. We now show that in the spinal cord, SIP30 was present in dorsal horn laminae where peripheral nociceptive inputs first synapse, colocalizing with nociception-related neuropeptides CGRP and substance P. With the onset of neuropathic pain after CCI surgery, SIP30 mRNA and protein levels increased in the ipsilateral side of the spinal cord, suggesting a potential association between SIP30 and neuropathic pain. When CCI-upregulated SIP30 was inhibited by intrathecal antisense oligonucleotide administration, neuropathic pain was attenuated. This neuropathic pain-reducing effect was observed both during neuropathic pain onset following CCI, and after neuropathic pain was fully established, implicating SIP30 involvement in the development and maintenance phases of neuropathic pain. Using a secretion assay in PC12 cells, anti-SIP30 siRNA decreased the total pool of synaptic vesicles available for exocytosis, pointing to a potential function for SIP30. These results suggest a role of SIP30 in the development and maintenance of peripheral nerve injury-induced neuropathic pain.

Send proofs to: Lei Yu, Department of Genetics and Center of Alcohol Studies, Rutgers University, 607 Allison Road, Piscataway, New Jersey 08854, USA; tel: 732-445-0794, fax: 732-445-3500, lei.yu@rutgers.edu.
*Equal contribution
¶Co-corresponding authors

Red font denotes the changes that have been made to the text of the original submission

Keywords

SIP30; neuropathic pain; chronic constriction injury; spinal cord; intrathecal; dorsal horn

1. Introduction

Neuropathic pain is a chronic and persistent painful condition, originating from nerve damage or dysfunction. Different from somatic pain that tends to subside after the injury heals, neuropathic pain often continues long after the initial injury has healed, and may persist in the absence of observable tissue damage. Effective alleviation of neuropathic pain remains clinically challenging, since neuropathic pain is refractory to the available therapeutic means in many patients [1,4,5,12]. Indeed, a recent survey of treatment options for neuropathic pain noted that “existing pharmacologic treatments for neuropathic pain are limited, with no more than 40–60% of patients obtaining partial relieve of their pain” [14]. To develop more effective therapeutic approaches, it is crucial to understand the mechanistic basis for neuropathic pain, and to identify molecules involved in the development and maintenance of neuropathic pain.

SIP30 is a SNAP25 (synaptosome-associated proteins of 25 kDa) interacting protein of 30 kDa [23]. This novel protein of 266 amino acids, like all SNAREs (soluble N-ethylmaleimide-sensitive factor attachment protein receptors), has a coiled-coil domain that forms a key component in protein-protein interactions [11,23,31]. SNAREs, including t-SNAREs (localized to the target membrane, grouped into the synaptosome-associated proteins of 25 kDa, and syntaxin families) and v-SNAREs (localized to the membrane of the trafficking vesicle, comprised by vesicle-associated membrane proteins, VAMP) are essential for regulated exocytosis of synaptic vesicles during neurotransmission [7,8,15,32,35]. SIP30 has been detected in various brain areas [23,26]. However, molecular and cellular functions for SIP30 remain unknown so far. In this study, we present evidence for a functional role of SIP30 in the development and maintenance of neuropathic pain, using the chronic constriction injury (CCI) model.

2. Methods

2.1. Animals

Adult male Sprague-Dawley rats, weighing 200–280 g, were housed in climate-controlled rooms with a 12:12 hr light/dark cycle, with food and water available ad libitum. All experimental protocols and animal handling procedures were approved by the Institutional Animal Care and Use Committee (IACUC) at the University of Cincinnati and the Animal Care and Facilities Committee at the Rutgers University, adhered to the guidelines of the Committee for Research and Ethical Issues of IASP, and were consistent with the National Institutes of Health Guide for the Care and Use of Laboratory Animals.

2.2. Intrathecal cannula implantation

Under sodium pentobarbital (45 mg/kg, i.p.) anesthesia, an intrathecal catheter (PE-10 tubing) was inserted through the space between the L4 and L5 vertebrae and extended to the subarachnoid space of the lumbar enlargement (L4 and L5 segments) of the rat spinal cord. The catheter was filled with sterile saline (approximately 4 μl), and the external end was closed. Cannulated rats were allowed to recover for 4 days and were housed individually. Rats that showed any neurological deficits resulting from the surgical procedure were excluded from the experiments.

2.3. Chronic constriction injury (CCI) of the sciatic nerve

Rats were anesthetized with pentobarbital sodium (45 mg/kg i.p.), and the right sciatic nerve was exposed at the mid-thigh level by blunt dissection of the biceps femoris. For CCI, four ligatures with chromic gut (4-0) were tied loosely around the nerve at approximately 1 mm apart, proximal to its trifurcation, as previously described [6,30,40]. For sham surgery, the sciatic nerve was isolated but not ligated. After CCI or sham surgery, the overlying muscles and skin were closed in layers with 4-0 silk sutures.

2.4. Antisense oligonucleotides and delivery

Oligonucleotides, including an antisense sequence (AS, 5′-TTT CTC CGC GTC CGC CAT GGT –3′) complementary to nucleotides 11–31 of the coding region of the rat SNAP25 interacting protein 30 (SIP30, GenBank accession number BC063144), and a corresponding missense sequence (MM, 5′-TTT CCT CGC GTC CCG CAT GGT- 3′), were obtained from Integrated DNA Technologies, Inc. (Coralville, IA). All of the oligonucleotide sequences were examined against the GenBank database using the BLAST algorithm to exclude non-specific match with any unintended nucleotide sequences. The oligonucleotides were reconstituted in 0.9 % normal saline (NS) before administration. Rats received intrathecal administration of normal saline (10 μl), antisense oligonucleotide (50 μg/10 μl), or missense oligonucleotide (50 μg/10 μl), respectively, followed by 5 μl of normal saline for flushing, every 24 hrs for 4 days (delivering protocol I: from day 0 (6 hrs before CCI surgery) to day 3 post-CCI surgery; delivering protocol II: from day 4 to day 7 post-CCI surgery).

2.5. Antibodies

Antibodies were made to amino acids 65–266 and 140–233 of SIP30 in rabbits as previously described [23]. In addition, A GST-tagged SIP30 full-length sequence was inserted in-frame into the pGEX-4T-1 vector (GE Health Life Science) at the BamHI and EcoRI cloning sites. The resulted plasmid clone expressed a ~60kd protein which was identified as GST-SIP30 by anti-GST. The GST-SIP30 was purified with glutathione Sepharose 4B (Amersham Pharmacia Biotech, Piscataway, NJ) and was used as the antigen to raise antisera from 2 rabbits. The specificity of antisera was determined by Western blotting and immunohistochemical staining with proteins from SIP30-transfected 293-T cells, using the pre-immune serum as the control.

2.6. Immunohistochemical staining

Immunohistochemical staining was performed as previously described [16]. Briefly, rats were deeply anesthetized with sodium pentobarbital (120 mg/kg, i.p.) and transcardially perfused with 50–100 ml of warm saline with heparin sodium, followed by 400 ml of 4% paraformaldehyde. The L5 DRGs and the L4 and L5 segments of the spinal lumbar enlargement were removed, post-fixed in the same fixative for 90 min, and then placed in 30% sucrose solution at 4°C overnight. Tissues were embedded with Leica OCT Cryocompound (Leica Microsystems, Nussloch, Germany), cut coronally in a cryostat at 15 μm thickness, and mounted onto gelatin-coated slides. Immunohistochemical staining was performed using the following antibodies: Primary antibodies against SIP30 or CGRP (1:2000, monoclonal, Sigma-Aldrich), Substance P (1:1000 Guinea pig, a gift from Dr. JiSong Guan), NF200 (1:100, Sigma-Aldrich) and FITC-IB4 (1:400, Sigma-Aldrich); FITC-, Cy3- and Cy5-conjugated secondary antibodies were obtained from Jackson ImmunoResearch Laboratories (West Grove, PA). Normal mouse and rabbit IgG (Zymed, South San Francisco, CA) were used as the negative control. Digital images were captured with a confocal microscope (TCS SP2, Leica, Heidelberg, Germany).

2.7. RNA isolation from spinal cord tissue and DRG

Rats were sacrificed on the 3rd or 7th day after CCI or sham surgery. In order to assess the development of neuropathic pain and effects of antisense oligonucleotide, rats were tested for both mechanical allodynia and thermal hyperalgesia as described before being sacrificed. The spinal cord from naïve, sham, or CCI rats was dissected and cut along the midsagital plane into two halves, one ipsilateral and one contralateral to the CCI surgery side. The DRG tissues (L4–L6) from the same animals were also dissected. After dissection, all tissues were rapidly frozen in dry ice and stored at −80 °C until further processing. Frozen spinal cord tissues were directly homogenized in 1 ml TRIZOL reagent (Invitrogen, Carlsbad, CA). Total RNA was extracted following manufacturer's protocol with minor modifications. Briefly, following chloroform extraction, RNA was precipitated with isopropanol and the pellet washed two times in 70% ethanol. After air drying, RNA was resuspended in DNase/RNase-free water. Both the quality and quantity of the total RNA were examined by gel electrophoresis and by UV absorption measurements (Agilent 2001 Bioanalyzer, Palo Alto, CA). Extracted RNA was treated with DNase I (DNA-free, Ambion) to remove genomic DNA. cDNA was synthesized with random decamers using the Ambion RETROscript reverse transcription kit according to the manufacturer's instructions. Negative control reactions were run without RNA template to test for contamination of reagents.

2.8. Real-time PCR

Real-time PCR analysis was performed on a Cepheid Smart Cycler. Threshold cycles (Ct) were calculated using the Smart Cycler Data Analysis Software 2.0 (Cepheid). PCR reaction was performed in a final volume of 20 μl using LightCycler DNA Master SYBR Green I kit containing: 12.6 μl of PCR grade water, 2.4 μl of $MgCl_2$ (25 mM), 2 μl of 10X LightCycler DNA Master SYBR Green I (Taq DNA polymerase, reaction buffer dNTP mix with dUTP instead of dTTP, SYBR Green I dye, and 10 mM $MgCl_2$), 2 μl of cDNA template, 0.5 μl of forward and reverse primer (100 ng/μl) respectively. The amplification protocol included 150 sec at 95 °C to activate the Taq DNA polymerase, then 40 cycles of 10 sec denaturation at 95 °C, 15 sec annealing at 58 °C, and 20 sec extension at 72 °C. Each sample was run in triplicates and Ct values were averaged. For controls, no-template reactions were run in which water replaced the cDNA template. In this study, β-actin was used as the reference gene to normalize expression levels. The relative gene expression level was computed from the target and β-actin using the following formula [3,24,27]: mRNA relative expression = $2^{-(\text{Ct of target} - \text{Ct of } \beta\text{-actin})}$. Primers were designed with Invitrogen Custom Primer Designer. The primer sequences are listed in Supplemental Table 1.

2.9. Protein extraction

Frozen spinal cord tissues were directly homogenized in 500 μl of lysis buffer containing 50 mM Tris-HCl, pH 7.5, 150 mM NaCl, 5 mM EDTA, 1% Triton, 1% SDS, 1 mM phenylmethylsulfonyl fluoride, 2 μg/ml aprotintin, 2 μg/ml leupeptin, and 2 μg/ml pepstain. Protein concentrations were determined by the Bradford method.

2.10. Western blotting

Twenty micrograms of total protein for each sample were separated by 10% SDS-PAGE, and were transferred onto polyvinylidene difluoride membranes. The membranes were blocked in 3% nonfat dry milk, and incubated overnight at 4 °C with an anti-SIP30 primary antibody (1:2000) against amino acids 65–266 of SIP30 [23]. Western blots were incubated for 1 hr at room temperature with a horseradish peroxidase (HRP)-conjugate secondary antibody (1:5000; Santa Cruz Biotechnology). Visualization of signals was aided with enhanced chemiluminescence (ECL, Amersham Biosciences), and the Western blots were exposed to X-ray films. The blots were then stripped in stripping buffer (67.5 mM Tris, pH 6.8, 2% SDS,

and 0.7% β-mercaptoethanol) for 30 min at 50 °C and reprobed with an antibody against β-actin (1:3000; Santa Cruz, Biotechnology) as the loading control. All Western blot analyses were performed at least three times, and similar results were obtained. Bands on Western blots were scanned and quantified using the Metamorph program.

2.11. Von Frey filament test of mechanical sensitivity

The hindpaw withdrawal threshold was determined using a series of von Frey filaments (Stoelting, IL) with calibrated bending force ranging from 0.6 to 18 g. Animals were placed individually in wire mesh-bottom cages, and allowed to acclimate for 30 min. Von Frey filaments were applied to the central region of the plantar surface of a hindpaw in ascending order of force (0.6, 0.9, 1.3, 2.2, 4.8, 6, 7.2, 9, 13, and 18 g). Testing was performed only when the rat was stationary and standing on all four paws. A withdrawal response was considered valid only if the hindpaw was completely lifted from the mesh-bottom. When a withdrawal response was established for a given animal, a von Frey filament with the next lower force was used to retest, until no response occurred. A trial consisted of applying a von Frey filament five times at 15 s intervals to each hindpaw. The hindpaw withdrawal threshold was defined as the lowest force that caused at least three withdrawals out of five consecutive applications. Once the threshold was determined for the left hindpaw, the same testing procedure was repeated on the right hindpaw of the same rat after 5 min.

2.12. Hargreaves test for thermal sensitivity

Thermal hyperalgesia was assessed by measuring the latency of paw withdrawal in response to a radiant heat source. Rats were placed individually into Plexiglas chambers on an elevated glass platform, and were allowed to acclimate to the test chamber. A radiant heat source (model 336 combination unit, IITC/life Science Instruments, Woodland Hill, CA) was applied from underneath the platform to the glabrous surface of the paw through the glass plate. When the rat lifted the hindpaw, the heat source was turned off, and the elapsed time was recorded; this was the hindpaw withdrawal latency. Throughout the testing, the heat intensity was maintained at a constant level, giving a consistent withdrawal latency of approximately 8–10 s in the absence of CCI. A 20 s cut-off was used to prevent tissue damage in the absence of a response. Rats were tested individually in groups of four, such that the stimulation was delivered once to the left hindpaw (control side) of each rat and then to the right hindpaw (CCI side) with a 5 min interval. This process was repeated two more times, and the values from the three trials for each hindpaw were averaged.

2.13. Motor activity testing

Locomotor activity was measured as previously described [33,39,41].

2.14. PC12 cell transfection and synaptic vesicle exocytosis assay

PC12 cells (ATCC) were seeded in poly-D-lysine coated 60-mm diameter Petri dish at a density of 3×10^6 cells/dish, with DMEM high glucose culture medium (Sigma-Aldrich) supplemented with 6.5% FBS (Lifeblood Medical Inc.), and 6.5% horse serum (Hyclone). siGENOME SMARTpool siRNA for both SIP30 and universal control were from Dharmacon. One day after seeding, cells were transfected with pHGH-CMV5 plasmid, which expresses human growth hormone [9,37], plus either the universal control siRNA or the SIP30 siRNA. One day after transfection, PC12 cells were harvested, and were reseeded into 6 wells of a 12-well plate. Two days after reseeding, PC12 cells were subject to secretion assay. Of the 6 wells of cells for each sample, cells from 3 wells were used for measuring baseline growth hormone secretion, and those from the other 3 wells were used to measure stimulated secretion.

Secretion assay to determine synaptic vesicle exocytosis was carried out as previously described [9,37] with some modifications. Briefly, culture medium was removed by aspiration, and PC12 cells were washed with pre-warmed PBS. For measuring baseline secretion, 500 μl of low K^+ PSS buffer (5.6 mM KCl, 145 mM NaCl, 2.2 mM CaCl2. 0.5 mM MgCl2, 5.6 mM Glucose, 15 mM HEPES, pH 7.4) was added to each well. For measuring stimulated secretion, 500 μl of high K^+ PSS buffer (56 mM KCl, 95 mM NaCl, 2.2 mM CaCl2. 0.5 mM MgCl2, 5.6 mM Glucose, 15 mM HEPES, pH 7.4) was added to each well. Cells were incubated at 37°C in a CO_2 incubator for 15 min. The plate was then placed on ice, and the buffer was transferred to a 1.5 ml microcentrifuge tube. The microcentrifuge tubes were centrifuged for 5 min at 300 × *g* to pellet any dislodged cells, and the supernatant was transferred to a fresh microcentrifuge tube for assay of secreted hormone. To the cells remaining in the well, an aliquot of 200 μl CelLyticM reagent (Sigma-Aldrich) was added to each well, and the plate was placed on ice on an orbital shaker for 10 min to lyse the cells. Cell lysate was transferred to the correspondence microcentrifuge tube with the pelleted cells. One milliliter PBS was added to each well to wash, and the solution was pooled with the correspondence cell lysate. The cell lysate was centrifuged at 14,000 rpm for 10 min to pellet cell debris, and the supernatant was transferred to a fresh microcentrifuge tube for assay of retained hormone in PC12 cells. The content of human growth hormone (hGH) was measured using the Roche hGH ELISA kit following the manufacturer's instructions. The percentage of hGH being secreted was calculated with the function hGHsecreted/(hGHsecreted+hGHretained) × 100% as an index of synaptic vesicle exocytosis.

2.15. Statistical analysis

Data were expressed as mean ± S.E.M. Data were analyzed for statistical significance by two way repeated measures analysis of variance [Two-way RM ANOVA (treatment × time)] with a pair-wise multiple comparison assessed with Turkey's test. $P<0.05$ was considered statistically significant.

3. Results

3.1. Identification of SIP30 as a candidate molecule involved in neuropathic pain in a rodent model

In an effort to uncover novel molecular components that are involved in modulating neuropathic pain, we used chronic constriction injury (CCI) as a rodent model of neuropathic pain [6,30,40], so as to look for differentially expressed genes in the spinal cord of the CCI rats. To identify genes that are involved in the early phase of the neuropathic pain, time course of neuropathic pain development after CCI surgery was determined in rats that had received unilateral CCI surgery (Supplemental Fig. 1). At 2-day post-CCI surgery, for the CCI hindpaw compared with the control hindpaw (i.e., no surgery), both thermal and tactile nociceptive thresholds were greatly decreased, to approaching almost maximum. These results are consistent with the previous studies that mechanical allodynia and thermal hyperalgesia developed within a few days following CCI [21]. Based on this time course information, we chose post-CCI day 3 as the time point, and isolated RNA from the lumbar enlargement portion of the control and CCI-surgery animals. Gene expression profiles were analyzed using a custom-constructed cDNA library as previously described [18,20,38]. We focused on those genes whose expression was elevated after CCI, of which a cDNA clone coding for SIP30 was identified in this process. SIP30 has been shown to be present in the rat brain and interact with SNAP25 [23], but its molecular function was unknown so far. Because our preliminary analysis showed increased expression of SIP30 with the onset of neuropathic pain in the CCI animals (data not shown), we chose SIP30 to further examine its potential role as a candidate molecule involved in neuropathic pain.

3.2. SIP30 mainly colocalizes with markers for small-diameter neurons

To evaluate SIP30 expression pattern in various CNS and peripheral tissues, Northern blot analysis was carried out, showing that SIP30 was mainly expressed in the CNS (Fig. 1A). These results corroborate with an earlier report [23].

Next, we examined the expression of SIP30 in the DRG. Small-diameter DRG neurons are primarily nociceptors. They can be divided neurochemically into two populations: isolectinB4 (IB4)-positive nonpeptidergic neurons, and IB4-negative peptidergic neurons. IB4 negative neurons express TrkA receptors for nerve growth factor (NGF), depend on NGF for survival, and contain neuropeptides such as calcitonin gene-related peptide and substance P. IB4 positive neurons express receptors for glial-derived neurotrophic factor (GDNF), neurturin, or artemin. IB4-positive and -negative nociceptors are functionally distinct [36]. It has been hypothesized that IB4-negative neurons contribute to inflammatory pain, whereas IB4-positive neurons contribute to neuropathic pain [10,25,34].

SIP30 expression was examined together with IB4 and CGRP in normal adult rats DRG (L4–L5). SIP30 is expressed almost entirely across small- to medium-diameter DRG neurons (Fig. 1B). SIP30 displayed an overlapping pattern with IB4 and CGRP in some neurons but mainly co-expressed with CGRP (Fig. 1B, panel d,e), suggesting a peptidergic nature. We also used large-diameter neuron marker NF200 in DRG staining (Fig. 1C, panel g,h), and found that SIP30 colocalized with very few large-diameter neurons (Fig. 1C, panel i).

SIP30 immunoreactivity was examined in the lumbar spinal cord, where it was found to be expressed in all lumbar levels and throughout all laminae. SIP30 immunoreactivity was particularly concentrated in the superficial dorsal horn lamina I and II (Fig. 1D, panel a), and showed a strong co-expression pattern with nociception-related neuropeptides CGRP and substance P (Fig. 1D, panels d,e,f). In addition, SIP30 immunohistochemical staining was present in cell bodies in laminae IV-VII as well as in motor neurons in the ventral horn.

3.3. Upregulation of SIP30 in the spinal cord following CCI

SIP30 mRNA was measured by quantitative real-time PCR, in both the spinal cord and DRG of either CCI or sham-operated rats. The expression levels of two other genes were used as reference points to normalize the amount of total RNA amount in each sample. We first examined the expression of β-actin and glyceraldehydes-3-phosphate dehydrogenase (GAPDH) among the normal and CCI rats' spinal cord and DRG using quantitative real-time PCR analysis. The β-actin and GAPDH gene expression levels of the CCI rats were normalized to those of the normal rats. We observed that β-actin expression was more consistent than GAPDH expression in the spinal cord and DRG (data not shown). Thus, β-actin was chosen as the reference in the present study. Both on day 3 and 7 post-CCI, a statistically significant ($p<0.05$) increase of SIP30 mRNA in the ipsilateral, but not contralateral spinal cord was observed in CCI rats compared to sham-operated or normal rats (Fig. 2A, upper panel). However, in the DRG, SIP30 mRNA expression was not significantly changed by CCI; there was no difference between the ipsilateral and contralateral DRG in either sham or CCI rats (Fig. 2A, lower panel).

The upregulation of SIP30 protein was also demonstrated by Western blot analysis. Increased levels of SIP30 were observed in ipsilateral lumbar spinal cord compared with the contralateral side of CCI rats and both sides of sham-operated animals (Fig. 2B). Similar to the expression of SIP30 mRNA in the DRG from CCI and sham-operated rats, no significant changes in SIP30 protein were found in DRG following CCI (Fig. 2C).

Spinal cord immunohistochemical staining indicated that SIP30 protein level was elevated in the ipsilateral side of the spinal cord dorsal horn 3 and 7 days after CCI (Fig. 2D). Quantification

of SIP30 expression level by the number of SIP30-IR cells (Fig. 2D, panel c) indicated a significant increase both in the superficial layers (laminae I–II) and deep layers (laminae IV–V) in the ipsilateral side of the dorsal horn. At high magnification, SIP30 immunoreactivity was observed in the cytoplasm, but not in the nucleus (Fig. 2D, panel d).

SIP30 localization in CCI spinal cord was examined, showing colocalization with NeuN, a neuronal marker, in the spinal dorsal horn, 3 days after CCI (Fig. 2E, panel a). SIP30 did not show overlap staining with either the microglial marker OX-42 (Fig. 2E, panel b) or the astrocytic marker GFAP (Fig. 2E, panel c).

These results indicated that during CCI, SIP30 levels were upregulated in the ipsilateral side of the spinal cord, suggesting a potential functional association between elevated SIP30 levels and neuropathic pain.

3.4. SIP30 is involved in the development and maintenance of neuropathic pain

Intrathecal administration of SIP30 antisense oligonucleotide (50 μg/10 μl, once a day for 4 days) starting on day 0 (6 hrs before CCI), produced a partial attenuation in the development of mechanical allodynia and thermal hyperalgesia by day 4 of SIP30 antisense oligonucleotide administration (Fig. 3). Two-way ANOVA showed a statistically significant difference between the antisense group and normal saline group ($p<0.05$). The antisense oligonucleotide-induced attenuation was reversible: two days after the cessation of antisense oligonucleotide administration (post-CCI day 5), mechanical allodynia was similar in the antisense oligonucleotide group and the normal saline group (Fig. 3A); on post-CCI day 7, thermal hyperalgesia appeared with similar paw withdrawal latencies to that of the normal saline group (Fig. 3B). Administration of missense oligonucleotide had no effect on the development of mechanical allodynia and thermal hyperalgesia. Contralateral paw withdrawal thresholds and latencies were not affected by antisense oligonucleotide, missense oligonucleotide, or normal saline treatment (Fig. 3C,D). Using another SIP30 antisense oligonucleotide (against nucleotides 143-162 of the coding region of the SIP30 gene) also showed similar attenuating effect on CCI-induced neuropathic pain (Supplemental Fig. 2).

By 3 d after CCI, animals developed both mechanical allodynia and thermal hyperalgesia. After this point of established neuropathic pain, 4 d of treatment with SIP30 antisense oligonucleotide resulted in an attenuation of neuropathic pain (Fig. 4). Two-way ANOVA showed a statistically significant difference between the antisense oligonucleotide group and the normal saline or missense oligonucleotide group on day 7 and 9 post-CCI ($p<0.05$, Fig. 4A,B). Four days after antisense oligonucleotide withdrawal, mechanical allodynia and thermal hyperalgesia reappeared. Neither missense oligonucleotide nor normal saline altered paw withdrawal responses to mechanical and thermal stimuli in CCI rats. There was no effect of normal saline, antisense oligonucleotide and missense oligonucleotide treatment on contralateral hindpaw during and post treatment period (Fig. 4C,D).

Treatment with SIP30 antisense oligonucleotide (50 μg/10 μl, once a day for 4 days) had no detectable effect on the responses of naïve rats to von Frey and thermal stimuli in both hindpaws ($p>0.05$, Fig. 5). Additionally, to rule out the possibility that intrathecal SIP30 antisense oligonucleotide may produce non-specific motor deficiencies, locomotor activities were measured in naïve rats receiving SIP30 antisense oligonucleotide, and no abnormal behavior or motor deficiencies were observed during treatment with SIP30 antisense oligonucleotide (data not shown).

Taken together, these findings showed that inhibition of upregulated SIP30 levels in the spinal cord resulted in attenuation of neuropathic pain behaviors both during the development process

and the maintenance phase of neuropathic pain, suggesting a cause-effect relation between SIP30 upregulation and the phenomenon of neuropathic pain.

3.5. SIP30 antisense oligonucleotide knock-down inhibits both SIP30 and SNAP25 expression in the spinal cord

Because SIP30 levels in the DRG did not change after CCI at either mRNA or protein level, in the subsequent experiments we focused only on the spinal cord. In order to verify whether intrathecal administration of SIP30 antisense oligonucleotide indeed resulted in knockdown of SIP30 over-expression, the effect of SIP30 antisense oligonucleotide on SIP30 mRNA and protein expression was assessed. SIP30 antisense oligonucleotide (50 μg/10 μl) and missense oligonucleotide (50 μg/10 μl) were administered intrathecally. The lumbar enlargement segments of the spinal cord were harvested at 6 hrs after the last injection. Quantitative real-time PCR showed that SIP30 antisense oligonucleotide significantly decreased the over-expression of SIP30 mRNA in the ipsilateral spinal cord compared with that by SIP30 missense oligonucleotide administration, for both day 0–3 and day 4–7 treatment procedures (Fig. 6A). Moreover, Western blot analysis showed that the SIP30 antisense oligonucleotide, but not the missense oligonucleotide, markedly suppressed the over-expression of SIP30 protein levels in the ipsilateral spinal cord for day 0–3 intrathecal administration procedure (Fig. 6B), further substantiating the antisense oligonucleotide-mediated “knockdown” of the over-expression of SIP30 protein. Antisense oligonucleotide only suppressed the CCI-induced over-expression of SIP30 on the ipsilateral side, and did not reduce the baseline levels of SIP30 mRNA or protein expression on the contralateral side (Fig. 6A,B), consistent with the observation that antisense oligonucleotide did not affect nociceptive behavior in normal animals (Fig. 5). This lack of adverse effect by antisense oligonucleotide on normal levels of gene expression has been reported for a sodium channel in a neuropathic pain study [17].

To assess whether SIP30 antisense oligonucleotide affects other protein factors that may interact with SIP30, we also examined two related synaptic proteins that are expressed in the spinal cord, synaptosome-associated proteins of 25 kDa (SNAP25), and postsynaptic density protein-95 (PSD95). As shown in Fig. 6C, PSD95 mRNA exhibited a significant upregulation in the ipsilateral spinal cord on day 7 post-CCI, and this upregulation of PSD95 mRNA was not blocked by SIP30 antisense oligonucleotide. On the other hand, SNAP25 mRNA in the ipsilateral spinal cord also showed a significant upregulation on both day 3 and 7 post-CCI, and this CCI-induced upregulation of SNAP25 mRNA was suppressed by SIP30 antisense oligonucleotide (Fig. 6D). As a cytological basis of interaction between SIP30 and SNAP25, double immunofluorescence staining indicated that SIP30 co-localized with SNAP25 in terminals of spinal dorsal horn neurons (Fig. 7).

3.6. SIP30 inhibition resulted in reduced synaptic vesicle exocytosis in PC12 cells

In an effort to identify cellular functions that SIP30 may be involved in, we considered its molecular interaction with SNAP25 as a potential lead. Several other SNAP25 interacting proteins have been identified with yeast two-hybrid screening by various investigators. SNAP25 contains coiled-coil domains known to mediate protein-protein interaction [11,29]. Some of these SNAP25 interacting proteins, such as SNIP, Snapin and Hrs (hepatocyte growth factor-regulated tyrosine kinase substrate), also contain coiled-coil domains, and their interactions with SNAP25 are mediated by the coiled-coil domains of both proteins [13,19, 22]. Since a major function of SNAP25 is the regulation of synaptic vesicle docking during exocytosis [2,28], we sought to examine SIP30 involvement in synaptic vesicle exocytosis.

Using a growth hormone secretion assay in PC12 cells [9,37], we first examined the effect of over-expression of SIP30. PC12 cells were either transfected with pHGH-CMV5 and pcDNA3 empty vector as the negative control, or with pHGH-CMV5 and pcDNA3-SIP30. Thirty-six

hrs after transfection, both baseline and stimulated secretion of hGH were assayed by incubating the cells in a low or high K^+ buffer, respectively. Our results indicated that vesicular exocytosis was not affected by over-expression of SIP30 (data not shown), even though a positive control plasmid over-expressing synaptogyrin1, a protein that was previous reported to inhibit stimulated secretion when over-expressed [37], did result in reduced vesicular exocytosis (data not shown). This may be due to the fact that PC12 cells already express relatively high levels of endogenous SIP30.

We next examined the effect of SIP30 inhibition, using an siRNA approach. PC12 cells were cotransfected either with the hGH plasmid and a control siRNA, or with the hGH plasmid and the SIP30 siRNA. As shown in Fig. 8, total vesicular hormone levels were significantly decreased by SIP30 siRNA treatment compared to the control ($p < 0.05$), and the baseline secreted hormone was also reduced ($p < 0.05$). These results indicated that the total pool of hormone-containing synaptic vesicles available for exocytosis was diminished by a reduced level of SIP30.

4. Discussion

The results of the present study pointed to SIP30 involvement in CCI-induced neuropathic pain. After CCI surgery, SIP30 levels were up-regulated in the spinal cord at both mRNA and protein levels (Fig. 2). It is noteworthy that CCI-induced up-regulation of SIP30 is restricted to the ipsilateral side of the spinal cord, not the contralateral side, suggesting specificity of the molecular change in correlation with CCI-induced neuropathic pain.

In addition to expression-level correlation with neuropathic pain, SIP30 also displayed a causal relationship with both the development and maintenance of neuropathic pain induced by CCI. With intrathecal SIP30 antisense oligonucleotide administration starting from the day of CCI surgery (days 0 of CCI surgery till day 4 post surgery), CCI-induced mechanical allodynia and thermal hyperalgesia were attenuated (Fig. 3; also Fig. 7), together with concomitant decrease of SIP30 mRNA and protein in the ipsilateral side of the CCI spinal cord (Fig. 6A,B). These data showed that inhibition of SIP30 over-expression at the time of nerve injury resulted in attenuated neuropathic pain, suggesting a causal relationship between SIP30 over-expression and the development of neuropathic pain. Furthermore, once neuropathic pain has established, intrathecal SIP30 antisense oligonucleotide administration also reduced mechanical allodynia and thermal hyperalgesia (Fig. 4), suggesting that the sustained elevation of SIP30 was also critical for the continued maintenance of neuropathic pain. Together, antisense knock-down experiments suggest that SIP30 is involved in both the development and maintenance of neuropathic pain in CCI rats.

One clue to a potential SIP30 function came from the synaptic vesicle exocytosis experiments. Inhibition of SIP30 by siRNA in PC12 cells resulted in much reduced neurotransmitter pool available for synaptic vesicle exocytosis (Fig. 8), suggesting that SIP30 may participate in modulating the steady-state neurotransmitter level in packed synaptic vesicles available for exocytosis in the presynaptic terminals. Previously, it has been shown that SIP30 is one of the molecules that are associated with SNAP25 [23]. Both SNAP25 and other SNAP25-associated SNAREs have been shown to be involved in synaptic vesicle exocytosis [2,13,19,22,28]. In this regard, the involvement of SIP30 in modulating synaptic neurotransmitter vesicle pool is suggestive of SIP30 being involved in the overall process of synaptic vesicle regulation. Additionally, it is noteworthy that SNAP25 mRNA over-expression was also reduced in the ipsilateral side of the spinal cord in the antisense knock-down experiments (Fig. 6D), even though the antisense oligonucleotide was against the SIP30 sequence. SNAP25 down-regulation appeared to be specific, since another synaptic density molecule, PSD95, was not affected by the SIP30 antisense oligonucleotide (Fig. 6C). To what extent such a co-regulation

of SIP30 and SNAP25 mRNA in the CCI spinal cord relates to their interaction and involvement in mediating neuropathic pain remains to be seen.

In conclusion, we identified a SNAP25-associated protein, SIP30, to be a molecule involved in both the development and maintenance of neuropathic pain in the CCI model. Intrathecal infusion of SIP30 antisense oligonucleotides significantly attenuated mechanical allodynia and thermal hyperalgesia during both the development and maintenance phase of chronic neuropathic pain, by knocking-down the levels of spinal SIP30, but not in DRG. These results suggest that SIP30 may be involved in the central mechanisms mediating chronic neuropathic pain, and that elevated levels of SIP30 may be necessary for the development and maintenance of allodynia and hyperalgesia induced by peripheral nerve injury.

Supplementary Material

Refer to Web version on PubMed Central for supplementary material.

Acknowledgments

We thank Dr. Thomas Sudhof and Dr. Mary Bittner for generously providing human growth hormone plasmids. This work was supported in part by grants from the National Institutes of Health of the United States (DA013471 and DA020555), the Life Science Special Fund of the Chinese Academy of Sciences for Human Genome Research (KJ95T-06 and KSCX1-Y02), the National Natural Science Foundation of China (30821002, 30870338, 30623003, 30721065, 30830034), the National Key Basic Research and Development Program of China (2007CB512303, 2007CB512502, 2006CB500807, 2005CB522704, 2006CB943902, 2007CB947101, 2008KR0695 and 2009CB941100), the Shanghai Key Project of Basic Science Research (06DJ14001, 06DZ22032 and 08DJ1400501), and the Council of the Shanghai Municipal for Science and Technology (088014199). The authors have no conflict of interest regarding this manuscript.

References

1. Arner S, Meyerson BA. Lack of analgesic effect of opioids on neuropathic and idiopathic forms of pain. Pain 1988;33:11–23. [PubMed: 2454440]
2. Banerjee A, Kowalchyk JA, DasGupta BR, Martin TFJ. SNAP-25 is required for a late postdocking step in Ca^{2+}-dependent exocytosis. J Biol Chem 1996;271:20227–20230. [PubMed: 8702751]
3. Beltramo M, Campanella M, Tarozzo G, Fredduzzi S, Corradini L, Forlani A, Bertorelli R, Reggiani A. Gene expression profiling of melanocortin system in neuropathic rats supports a role in nociception. Mol Brain Res 2003;118:111–118. [PubMed: 14559360]
4. Benedetti F, Vighetti S, Amanzio M, Casadio C, Oliaro A, Bergamasco B, Maggi G. Dose-response relationship of opioids in nociceptive and neuropathic postoperative pain. Pain 1998;74:205–211. [PubMed: 9520235]
5. Bennett GJ. Neuropathic pain: A crisis of definition? Anesth Analg 2003;97:619–620. [PubMed: 12933371]
6. Bennett GJ, Xie YK. A peripheral mononeuropathy in rat that produces disorders of pain sensation like those seen in man. Pain 1988;33:87–107. [PubMed: 2837713]
7. Bennett MK, Calakos N, Scheller RH. Syntaxin - a synaptic protein implicated in docking of synaptic vesicles at presynaptic active zones. Science 1992;257:255–259. [PubMed: 1321498]
8. Bennett MK, Garciaarraras JE, Elferink LA, Peterson K, Fleming AM, Hazuka CD, Scheller RH. The syntaxin family of vesicular transport receptors. Cell 1993;74:863–873. [PubMed: 7690687]
9. Bittner MA, Krasnoperov VG, Stuenkel EL, Petrenko AG, Holz RW. A Ca2+-independent receptor for alpha-latrotoxin, CIRL, mediates effects on secretion via multiple mechanisms. J Neurosci 1998;18:2914–2922. [PubMed: 9526008]
10. Breese NM, George AC, Pauers LE, Stucky CL. Peripheral inflammation selectively increases TRPV1 function in IB4-positive sensory neurons from adult mouse. Pain 2005;115:37–49. [PubMed: 15836968]

11. Chapman ER, An S, Barton N, Jahn R. Snap-25, a t-snare which binds to both syntaxin and synaptobrevin via domains that may form coiled coils. J Biol Chem 1994;269:27427–27432. [PubMed: 7961655]
12. Cherny NI, Thaler HT, Friedlanderklar H, Lapin J, Foley KM, Houde R, Portenoy RK. Opioid responsiveness of cancer pain syndromes caused by neuropathic or nociceptive mechanisms - a combined analysis of controlled, single-dose studies. Neurology 1994;44:857–861. [PubMed: 7514771]
13. Chin LS, Nugent RD, Raynor MC, Vavalle JP, Li L. SNIP, a novel SNAP-25-interacting protein implicated in regulated exocytosis. J Biol Chem 2000;275:1191–1200. [PubMed: 10625663]
14. Dworkin RH, O'Connor AB, Backonja M, Farrar JT, Finnerup NB, Jensen TS, Kalso EA, Loeser JD, Miaskowski C, Nurmikko TJ, Portenoy RK, Rice AS, Stacey BR, Treede RD, Turk DC, Wallace MS. Pharmacologic management of neuropathic pain: evidence-based recommendations. Pain 2007;132:237–251. [PubMed: 17920770]
15. Elferink LA, Trimble WS, Scheller RH. Two vesicle-associated membrane protein genes are differentially expressed in the rat central nervous system. J Biol Chem 1989;264:11061–11064. [PubMed: 2472388]
16. Gao X, Bian W, Yang J, Tang K, Kitani H, Atsumi T, Jing N. A role of N-cadherin in neuronal differentiation of embryonic carcinoma P19 cells. Biochem Biophys Res Commun 2001;284:1098–1103. [PubMed: 11414696]
17. Hains BC, Klein JP, Saab CY, Craner MJ, Black JA, Waxman SG. Upregulation of sodium channel Nav1.3 and functional involvement in neuronal hyperexcitability associated with central neuropathic pain after spinal cord injury. J Neurosci 2003;23:8881–8892. [PubMed: 14523090]
18. Hou Q, Gao X, Zhang X, Kong L, Wang X, Bian W, Tu Y, Jin M, Zhao G, Li B, Jing N, Yu L. SNAP-25 in hippocampal CA1 region is involved in memory consolidation. Eur J Neurosci 2004;20:1593–1603. [PubMed: 15355326]
19. Ilardi JM, Mochida S, Sheng ZH. Snapin: a SNARE-associated protein implicated in synaptic transmission. Nat Neurosci 1999;2:119–124. [PubMed: 10195194]
20. Jin M, Wang X-M, Tu Y, Zhang X-H, Gao X, Guo N, Xie Z, Zhao G, Jing N, Li B-M, Yu L. The negative cell cycle regulator, Tob, is a multifunctional protein involved in hippocampus-dependent learning and memory. Neurosci 2005;131:647–659.
21. Khalil Z, Liu T, Helme RD. Free radicals contribute to the reduction in peripheral vascular responses and the maintenance of thermal hyperalgesia in rats with chronic constriction injury. Pain 1999;79:31–37. [PubMed: 9928773]
22. Kwong J, Roundabush FL, Hutton MP, Montague M, Oldham W, Li Y, Chin LS, Li L. Hrs interacts with SNAP-25 and regulates Ca(2+)-dependent exocytosis. J Cell Sci 2000;113:2273–2284. [PubMed: 10825299]
23. Lee HK, Safieddine S, Petralia RS, Wenthold RJ. Identification of a novel SNAP25 interacting protein (SIP30). J Neurochem 2002;81:1338–1347. [PubMed: 12068081]
24. Livak KJ, Schmittgen TD. Analysis of relative gene expression data using real-time quantitative PCR and the 2(-Delta Delta C(T)) Method. Methods 2001;25:402–408. [PubMed: 11846609]
25. Mantyh PW, Hunt SP. Hot peppers and pain. Neuron 1998;21:644–645. [PubMed: 9808445]
26. Marie-Claire C, Courtin C, Robert A, Gidrol X, Roques BP, Noble F. Sensitization to the conditioned rewarding effects of morphine modulates gene expression in rat hippocampus. Neuropharmacology 2007;52:430–435. [PubMed: 17014870]
27. Marvizon JCG, McRoberts JA, Ennes HS, Song BB, Wang XR, Jinton L, Corneliussen B, Mayer EA. Two N-methyl-D-aspartate receptors in rat dorsal root ganglia with different subunit composition and localization. J Comp Neurol 2002;446:325–341. [PubMed: 11954032]
28. Mehta PP, Battenberg E, Wilson MC. SNAP-25 and synaptotagmin involvement in the final Ca(2+)-dependent triggering of neurotransmitter exocytosis. Proc Natl Acad Sci U S A 1996;93:10471–10476. [PubMed: 8816825]
29. Misura KM, Gonzalez LCJ, May AP, Scheller RH, Weis WI. Crystal structure and biophysical properties of a complex between the N-terminal SNARE region of SNAP25 and syntaxin 1a. J Biol Chem 2001;276:41301–41309. [PubMed: 11533035]

30. Moalem G, Xu K, Yu L. T lymphocytes play a role in neuropathic pain following peripheral nerve injury in rats. Neurosci 2004;129:767–777.

31. Mochida S. Protein-protein interactions in neurotransmitter release. Neurosci Res 2000;36:175–182. [PubMed: 10683521]

32. Oyler GA, Higgins GA, Hart RA, Battenberg E, Billingsley M, Bloom FE, Wilson MC. The identification of a novel synaptosomal-associated protein, SNAP-25, differentially expressed by neuronal subpopulations. J Cell Biol 1989;109:3039–3052. [PubMed: 2592413]

33. Richtand NM, Logue AD, Welge JA, Perdiue J, Tubbs LJ, Spitzer RH, Sethuraman G, Geracioti TD. The dopamine D3 receptor antagonist nafadotride inhibits development of locomotor sensitization to amphetamine. Brain Res 2000;867:239–242. [PubMed: 10837819]

34. Snider WD, McMahon SB. Tackling pain at the source: new ideas about nociceptors. Neuron 1998;20:629–632. [PubMed: 9581756]

35. Sollner T, Bennett MK, Whiteheart SW, Scheller RH. A protein assembly-disassembly pathway in-vitro that may correspond to sequential steps of synaptic vesicle docking, activation, and fusion. Cell 1993;75:409–418. [PubMed: 8221884]

36. Stucky CL, Lewin GR. Isolectin B(4)-positive and -negative nociceptors are functionally distinct. J Neurosci 1999;19:6497–6505. [PubMed: 10414978]

37. Sugita S, Janz R, Sudhof TC. Synaptogyrins regulate Ca^{2+}-dependent exocytosis in PC12 cells. J Biol Chem 1999;274:18893–18901. [PubMed: 10383386]

38. Wang X, Zhang Y, Kong L, Xie Z, Lin Z, Guo N, Strong JA, Meij JT, Zhao Z, Jing N, Yu L. *RSEP1* is a novel gene with functional involvement in neuropathic pain behavior. Eur J Neurosci 2005;22:1090–1096. [PubMed: 16176350]

39. Wu J, Zou H, Strong JA, Yu J, Zhou X, Xie Q, Zhao G, Jin M, Yu L. Bimodal effects of MK-801 on locomotion and stereotypy in C57BL/6 mice. Psychopharmacol 2005;177:256–263.

40. Xie W, Strong JA, Meij JT, Zhang JM, Yu L. Neuropathic pain: Early spontaneous afferent activity is the trigger. Pain 2005;116:243–256. [PubMed: 15964687]

41. Yates JW, Meij JT, Sullivan JR, Richtand NM, Yu L. Bimodal effect of amphetamine on motor behaviors in C57BL/6 mice. Neurosci Lett 2007;427:66–70. [PubMed: 17920769]

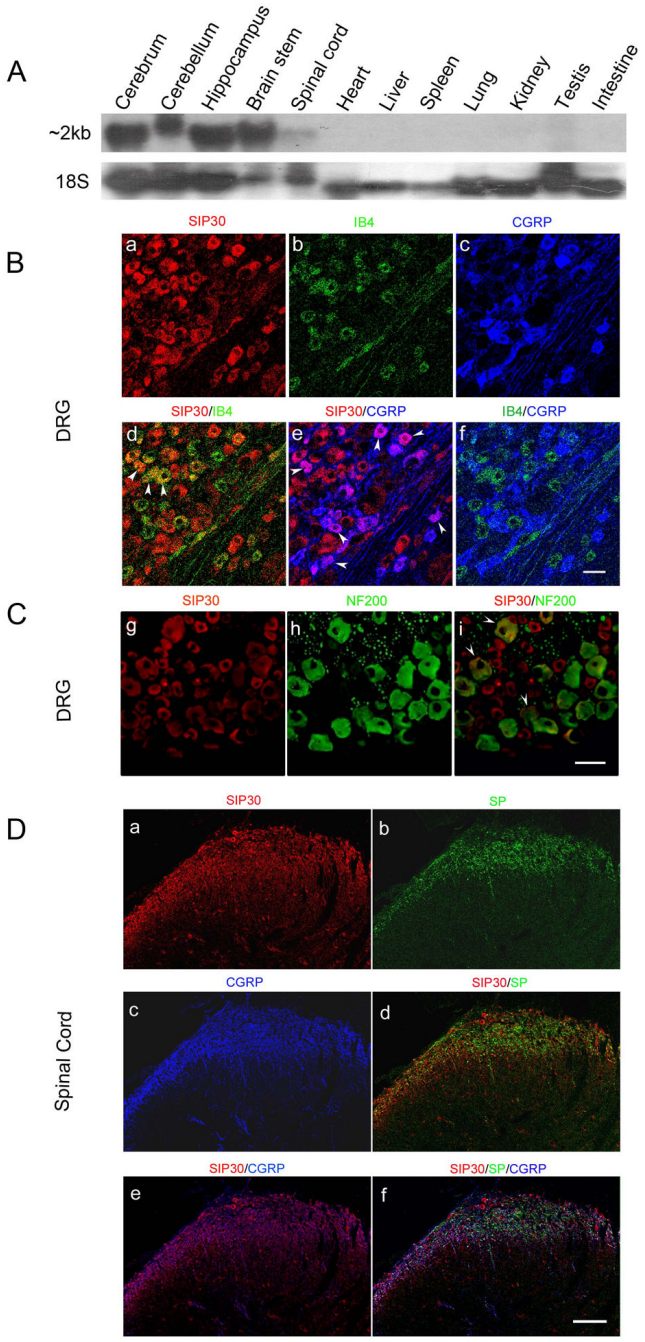

Fig. 1.

Expression pattern of SIP30 in normal rats. Scale bars, 50 μm. A, Northern blot analysis of SIP30 expression in various rat tissues. The 2 kb mRNA band of SIP30 was shown in the upper panel, and 18S ribosomal RNA (lower panel) was used as an internal control for sample loading. Source of tissue for RNA was indicated across the top for each lane. B, SIP30 levels in small-diameter neurons in the DRG. Immunological staining using antibodies against SIP30 (a), IB4 (b), and CGRP (c). Pair-wise superimposed composite images are shown as follows: SIP30 with IB4 (d), SIP30 with CGRP (e), and IB4 with CGRP (f). White arrowheads mark the cells with double staining. C, SIP30 levels in large-diameter neurons in the DRG. Immunological staining using antibodies against SIP30 (g) and NF200 (h). As seen in the merged image (i),

only a few large-diameter neurons showed colocalization with SIP30 (white arrowheads mark the cells with double staining). D, SIP30 levels in the spinal cord. Immunological staining using antibodies against SIP30 (a), substance P (b), and CGRP (c). Superimposed composite images are shown as follows: SIP30 with substance P (d), SIP30 with CGRP (e), and triple composite of SIP30 with substance P and CGRP (f).

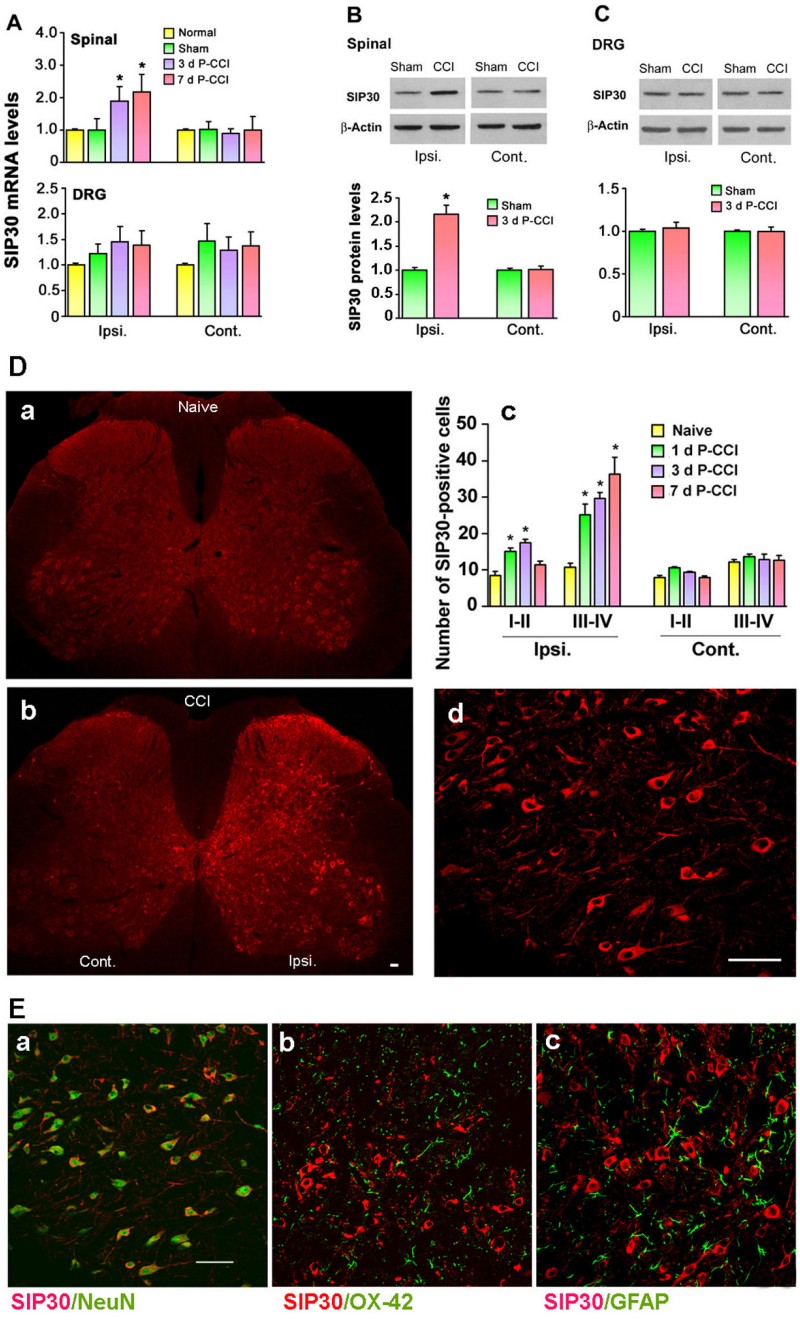

Fig. 2. SIP30 was up-regulated during CCI

A, SIP30 mRNA levels in the spinal cord (upper panel) and DRG (lower panel). Real-time PCR amplification results for SIP30 mRNA are shown relative to the mean levels in normal animals. Spinal cord tissues from rats receiving no surgery (normal), sham-CCI surgery (sham), or CCI surgery (3 days and 7 days post surgery, respectively) were collected, and RNA was isolated from the ipsilateral and contralateral side of the sham or CCI surgery for real-time PCR analysis. *, significant difference ($p < 0.05$ vs. normal or sham group) in the ipsilateral but not contralateral spinal cord for both day 3 and day 7 after CCI surgery. No significant difference was observed in DRG.

B, Western blot analysis of SIP30 protein levels in the spinal cord. Spinal cord tissues from rats receiving sham or CCI surgery (3 days post surgery) were collected, and protein was isolated from the ipsilateral and contralateral side of the sham or CCI surgery for Western blot analysis. Upper panel, representative Western blots of SIP30 protein. β-Actin was used as the internal control. Lower panel, quantitative results of SIP30 protein. *, significant difference ($p < 0.05$ vs. sham group) for the ipsilateral side of the spinal cord.

C. Western blot analysis of SIP30 protein levels in DRG. DRG tissues from rats receiving sham or CCI surgery (3 days post surgery) were collected, and protein was isolated from the ipsilateral and contralateral side of the sham or CCI surgery for Western blot analysis. Upper panel, representative Western blots of SIP30 protein. β-Actin was used as the internal control. Lower panel, quantitative results of SIP30 protein. No significant difference was observed on either ipsilateral or contralateral side of DRG.

D, SIP30 protein level was elevated in the ipsilateral side of spinal cord dorsal horn after CCI. (a) Immunofluorescence shows basal expression of SIP30-IR cells in naïve rats; (b) Immunofluorescence indicates an increase in SIP30-IR cells in the dorsal horn on the ipsilateral side; (c) quantification of SIP30 expression level, as indicated by the number of SIP30-IR cells (per 30 μm section) in the superficial (laminae I–II) and deeper (laminae IV–V) dorsal horn; (d) A high magnification image showing SIP30 immunoreactivity in the cytoplasm but not nucleus. Scale bars, 50 μm.

E, Double immunofluorescence reveals that SIP30 (red) co-localized with NeuN (neuronal marker, green) (a), but dose not co-localize with OX-42 (microglial marker, green) (b) or GFAP (astrocytic marker, green) (c), in the dorsal horn of the spinal cord. Scale bar, 50 μm.

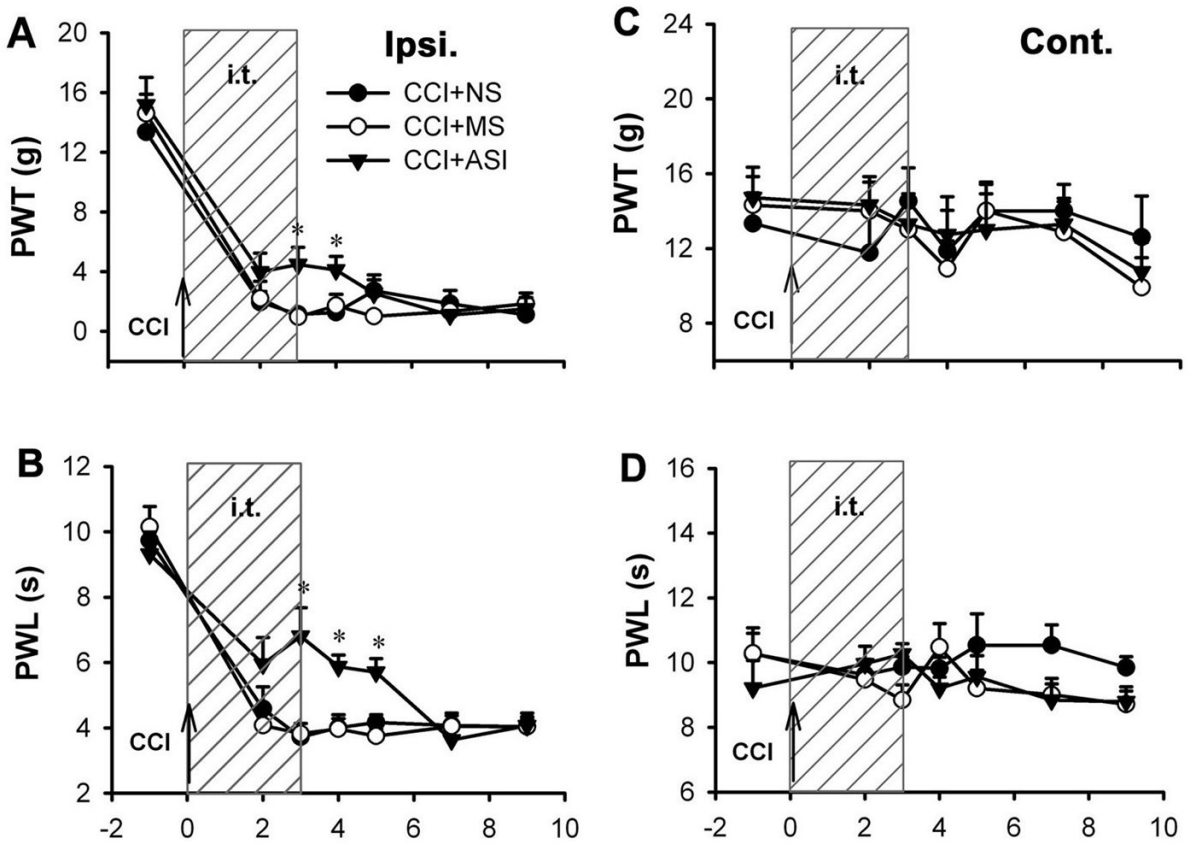

Fig. 3.

SIP30 participates in the development of peripheral nerve injury-induced neuropathic pain. Antisense oligonucleotide treatment was initiated on the day of CCI surgery, before the development of neuropathic pain. Shaded area (marked “i.t.”) indicates the duration of intrathecal injection. Upward arrow marked “CCI” indicates the day of CCI surgery. PWT, paw withdrawal threshold; PTL, paw withdrawal latency. Following the intrathecal injection of SIP30 antisense oligonucleotide (CCI+ASI) for 4 days (from day 0 to day 3 post-CCI), the development of mechanical allodynia (A) and thermal hyperalgesia (B) was attenuated in the CCI ipsilateral paw (“Ipsi.”), whereas normal saline (CCI+NS) and missense oligonucleotide (CCI+MS) had no effect. *$p<0.05$ for the SIP30 antisense oligonucleotide group vs. either normal saline or missense oligonucleotide group. (C, D) No significant change was seen in the CCI contralateral paw (“Cont.”) after the same treatments.

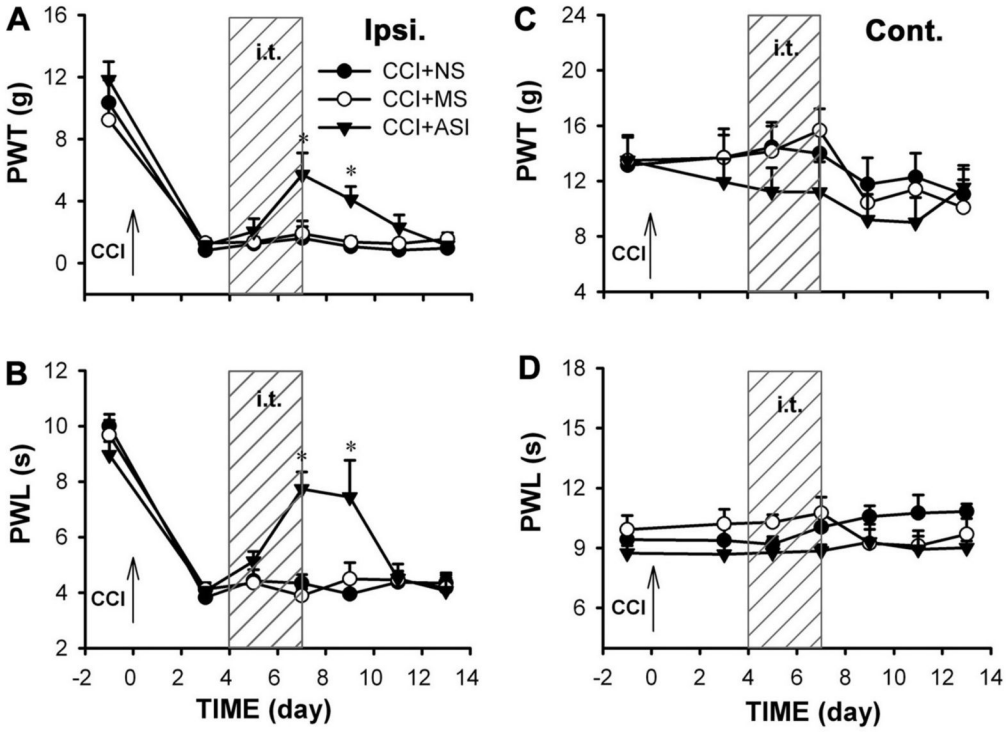

Fig. 4.

SIP30 participates in the maintenance of peripheral nerve injury-induced neuropathic pain. After mechanical allodynia and thermal hyperalgesia were already developed post CCI surgery, antisense oligonucleotide treatment was initiated. Shaded area (marked "i.t.") indicates intrathecal injection. Upward arrow marked "CCI" indicates the day of CCI surgery. PWT, paw withdrawal threshold; PTL, paw withdrawal latency. Intrathecal injection of SIP30 antisense oligonucleotide (CCI+ASI) for 4 days (from day 3 to day 7 post-CCI) attenuated both mechanical allodynia (a) and thermal hyperalgesia (b) in the CCI ipsilateral paw ("Ipsi."), but normal saline (CCI+NS) and missense oligonucleotide (CCI+MS) had no effect. *$p<0.05$ for the SIP30 antisense oligonucleotide group vs. either normal saline or missense oligonucleotide group. (c, d) No significant change was seen in the CCI contralateral paw after the same treatments.

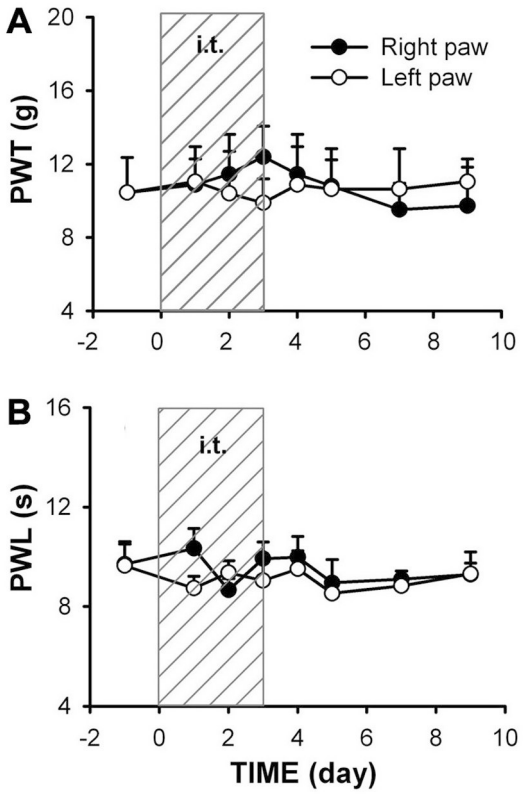

Fig. 5.

Treatment of SIP30 antisense oligonucleotide does not affect basal nociceptive response in control animals. In surgery-naïve rats, intrathecal injection of SIP30 antisense oligonucleotide for 4 days did not affect the basal responses to either von Frey (a) or thermal stimuli (b) in either paw. Shaded area (marked “i.t.”) indicates intrathecal injection. PWT, paw withdrawal threshold; PTL, paw withdrawal latency.

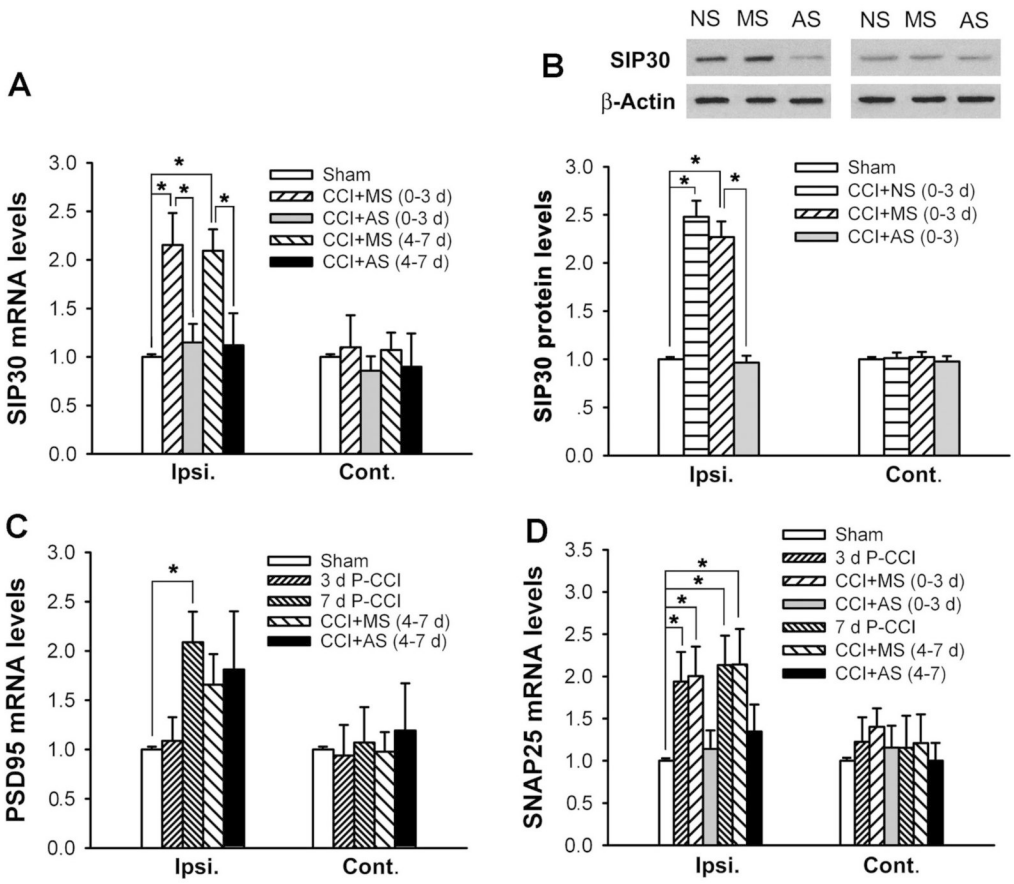

Fig. 6.

SIP30 antisense oligonucleotide knock down of SIP30 and SNAP25 levels. Abbreviations: NS, normal saline; AS, antisense oligonucleotide; MS, missense oligonucleotide. (0–3 d) indicates that rats received daily intrathecal injection from day 0 (6 hrs before CCI surgery) to day 3 post-CCI; (4–7 d) indicates that rats received daily intrathecal injection from day 4 to day 7 post-CCI.

A, SIP30 mRNA was increased after CCI, and the increase was reduced by antisense oligonucleotide. After four times of intrathecal administration of SIP30 antisense (AS) or missense (MS) oligonucleotide, rats were sacrificed and the lumbar spinal cords were dissected at six hours after the last injection. Real-time PCR amplification for SIP30 mRNA showed a significant decrease in the ipsilateral spinal cord in CCI rats receiving SIP30 antisense oligonucleotide compared with animals receiving missense oligonucleotide. *, significant difference ($p < 0.05$).

B, Western blot for SIP30 protein indicated a significant decrease in ipsilateral spinal cord in CCI rats receiving SIP30 antisense oligonucleotide compared with animals receiving missense oligonucleotide or normal saline. Upper panel, representative Western blots of SIP30 protein. β-Actin was used as the internal control. Lower panel, quantitative results of SIP30 protein. *, significant difference ($p < 0.05$).

C, Real-time PCR amplification for PSD95 mRNA showed a significant increase in ipsilateral spinal cord after CCI surgery. Intrathecal injection of SIP30 antisense oligonucleotide every 24 hours for 4 times did not appreciably affect PSD95 mRNA levels. *, significant difference ($p < 0.05$).

D, Real-time PCR amplification for SNAP25 mRNA showed a significant increase in ipsilateral spinal cord after CCI surgery. Intrathecal injection of SIP30 antisense

oligonucleotide every 24 hours for 4 times caused a trend to decrease in SNAP25 mRNA in ipsilateral spinal cord of CCI rats, although that did not reach statistical significance. *, significant difference ($p < 0.05$).

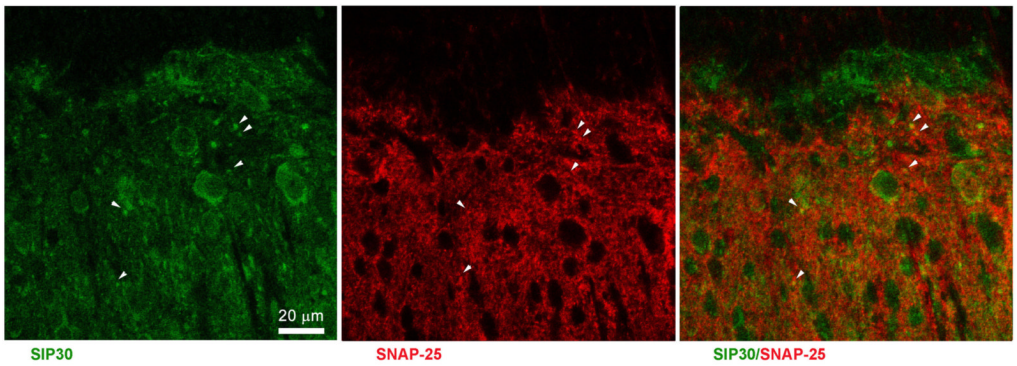

Fig. 7.

Double immunofluorescence staining shows that SIP30 (green) co-localized with SNAP-25 (red) in the dorsal horn of the spinal cord. Left panel: SIP30 immunoreactivity was present in both soma and terminals of spinal dorsal horn neurons. Middle panel: SNAP-25 immunoreactivity was present in presynaptic terminals of spinal dorsal horn neurons. Right panel: SIP30 (green) co-localized with SNAP-25 (red) in terminals of spinal dorsal horn neurons. Arrowheads indicate double-labeled terminals.

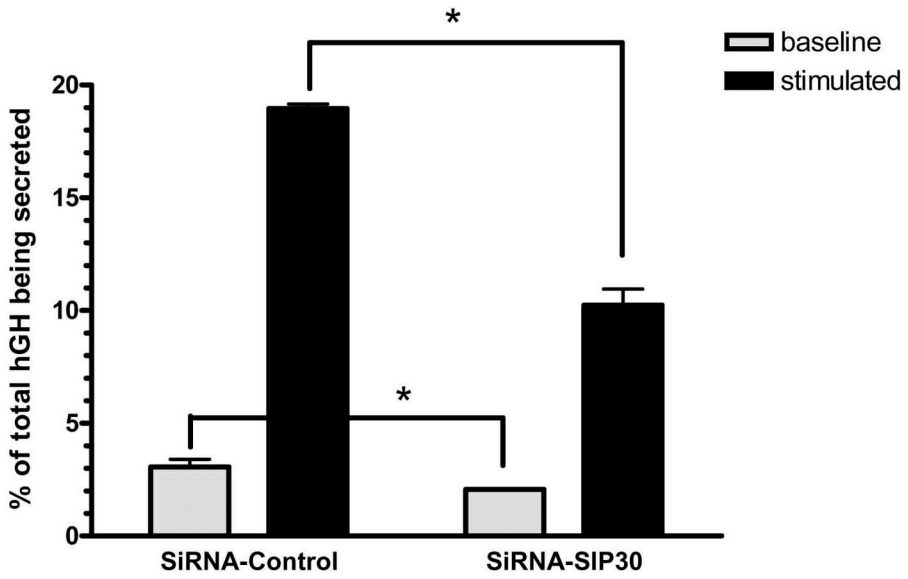

Fig. 8.

SIP30 siRNA inhibition of synaptic vesicle exocytosis in PC12 cells. Using human growth hormone (hGH) secretion in PC12 cells as an assay for synaptic vesicle exocytosis, cells were co-transfected with a hGH-coding plasmid plus either the control or anti-SIP30 siRNA oligonucleotides, and baseline secreted (grey bars) vs. total secretable hGH (filled bars) were measured. *, significant difference ($p < 0.05$, unpaired t test).